



## Tuning the Morphological and Optical Characteristics of SnO<sub>2</sub>/ZrO<sub>2</sub> Nanomaterials Doped PEO for Promising Optoelectronics Applications

Musaab Khudhur Mohammed<sup>1</sup>, Taif Nabeel Khudhair<sup>2</sup>, Khansaa Saleem Sharba<sup>2</sup>, Ahmed Hashim<sup>1\*</sup>, Qunoot Mohammed Hadi<sup>1</sup>, Mohanad H. Meteab<sup>2</sup>

<sup>1</sup> Department of Physics, College of Education for Pure Sciences, University of Babylon, Babylon 51002, Iraq

<sup>2</sup> Directorate General of Education in Babylon Governorate, Ministry of Education, Baghdad 10011, Iraq

Corresponding Author Email: [ahmed\\_taay@yahoo.com](mailto:ahmed_taay@yahoo.com)

Copyright: ©2024 The authors. This article is published by IIETA and is licensed under the CC BY 4.0 license (<http://creativecommons.org/licenses/by/4.0/>).

<https://doi.org/10.18280/rcma.340411>

### ABSTRACT

**Received:** 17 February 2024

**Revised:** 29 February 2024

**Accepted:** 1 July 2024

**Available online:** 27 August 2024

#### Keywords:

PEO, SnO<sub>2</sub> and ZrO<sub>2</sub> NPs, OM, optical properties, optoelectronic devices

In this work, the casting method was utilized to form the PEO/SnO<sub>2</sub>/ZrO<sub>2</sub> nanocomposite to improve its structural and optical characteristics. The formation network path inside the polymeric matrix at the higher concentration of nanoparticles was confirmed by the optical microscope (OM). The nanocomposite of PEO/SnO<sub>2</sub>/ZrO<sub>2</sub> has a higher absorbance in the UV region, which proved from the optical measurements that it can be used as an optoelectronic device. Increasing the concentration of SnO<sub>2</sub> and ZrO<sub>2</sub> NPs alters several properties. For example, the refractive index, optical conductivity, absorbance, extinction coefficient, and real and imaginary dielectric constants all increase, but the transmittance and energy optical band gap decrease. For the permitted and prohibited indirect transitions separately, the energy gap shrank from 3.68 eV to 3.4 eV and 3.66 eV to 3.35 eV, respectively. The narrowing of the energy band gap is very useful for many fields that work with optical devices.

## 1. INTRODUCTION

Nanotechnology is a nascent technology. The current generation is exerting a big impact on the global economy by developing innovative and substantial products, enhancing product utilization, and implementing more efficient production methods. Nanotechnology yields several types of nanoparticles, encompassing metallic, metal oxide, doped metallic, and undoped metallic and metal oxide particles. Nanoparticles are materials with dimensions between 1 and 100 nanometers in at least one direction. Within that narrow range, materials display distinct mechanical, chemical, and physical properties [1]. Due to their unique properties, polymer nanocomposites are becoming more popular [2]. Metal and semiconductor nanoparticles have excellent optical and electrical properties, making polymers good host materials [3]. Due to their remarkable features and new methods, nanocomposites with inorganic and organic components have gained technological strength in linear and nonlinear optics and solar cells [4]. Polymers behave like inorganic materials. However, polymers offer flexibility, simplicity of processing, corrosion resistance, affordability, and a lightweight composition. Thermal stability and structural integrity are also advantages of inorganic materials. In solar cell batteries, sensors, and TVs, polymer-inorganic hybrids find application [5].

The distinctive properties and wide range of applications of polyethylene oxide (PEO), a well-known synthetic polymer, have piqued the interest of researchers all over the globe. At

the very end of each polymer chain are hydrogen and hydroxyl groups. Hydrophobic ethylene groups and hydrophilic oxygen groups form a hydrogen bond site in the repeating unit [6]. Combining PEO with a catalyst achieves polymerization, resulting in PEO [7]. Because it is hydrophilic, linear, and lacks cross-links, it dissolves effectively in organic and water-based solvents [8]. At temperatures below 100°C, PEO dissolves easily in water, irrespective of the polymerization ratios or levels [9]. The properties of polyethylene oxide (PEO) include not being ionic, not being poisonous, not irritating, being biodegradable, and being biocompatible. Not only that, but the material is cheap [10]. There's a chance that PEO is a hybrid polymer with both amorphous and crystalline parts [11]. The physical features of this substance are exceptional, and they include qualities like high viscosity, low melting point (69°C), glass transition temperature (-50°C), flexibility, high ionic conductivity, and outstanding chemical stability [12].

Recently developed composites include carbides, metals, oxides, ionic materials, and biomaterials [13]. Tin oxide, a widely used and studied crystalline n-type semiconductor with a wide band gap, has been extensively researched. Researchers have extensively studied tin oxide gas sensors, dye-sensitized solar cells, optical, optoelectronic, and hybrid microelectronic devices [14]. Recent research suggests the chemical could be a lithium cell and photocatalysis electrode [14]. This oxide is a popular white pigment for conducting coatings due to its semi-conductive transparency. Tin oxide nanoparticles are synthesized using co-precipitation, hydrothermal, sol-gel, nonchemical polymer, and precursor techniques [15]. An n-

type semiconductor oxide, tin dioxide, has a wide bandgap. As a catalyst, catalytic support, biological and pharmaceutical gas sensor, rechargeable Li battery, and optical electronic device, tin dioxide (SnO<sub>2</sub>) has received attention. Gold-tin dioxide catalytic activity has garnered attention recently. In the research of Xavier et al. [16], nanocomposites showed excellent catalytic activity for CO oxidation at low temperatures. Tin dioxide (SnO<sub>2</sub>) finds wide applications as a catalyst, catalytic support, biological material, medicinal substance, gas sensor, rechargeable lithium battery component, and optical electronic gadget, contributing to its popularity. Gold-tin dioxide catalytic activity has garnered attention recently. In CO oxidation at low temperatures, nanocomposites were highly catalytic [17].

Zirconium oxide (ZrO<sub>2</sub>) is one of the most extensively studied transition metal oxides in the field of optics. In the visible and near-infrared spectrum, ZrO<sub>2</sub> films exhibit remarkable transparency, a large optical band gap, and a high refractive index [18]. Zirconia, or ZrO<sub>2</sub>, is a mineral with remarkable physical and chemical characteristics. Some of its many applications include catalysts, fuel cells, gas sensors, optoelectronics, and materials that resist corrosion [19-23]. ZrO<sub>2</sub> exhibits both illumination and high transparency [24]. Its large surface area, oxygen vacancies, and bandgap of more than 5 eV make it a promising photocatalytic candidate. Crystals in this material can be either cubic or tetragonal. Factors such as flaws, synthesis, particle size, and calcination temperature cause these variations in structure. The occurrence of phases at various calcination temperatures has been the subject of contradictory research [25].

Many studies have examined the optical characteristics of polymer composites with PEO as the host material. Al-Mehmadi et al. [26] added several proportions of tungsten trioxide (WO<sub>3</sub>) nanoparticles to PEO-NaAlg's research, which indicates that the presence of WO<sub>3</sub> leads to a decrease in the optical band gap. Al-Harbi et al. [27] did an independent study that showed that adding ZnO/GO nanostructured additives to PEO/CMC host polymers results in a substantial decrease in the bandgap. Moreover, previous studies have discovered changes in the optical band gap and refractive indices of PEO when it is filled with various dopants. The metal oxide had been into polymers to improve their optical properties [28-34].

The goal of this study is to make PEO/SnO<sub>2</sub>/ZrO<sub>2</sub> nanocomposites and look into their structure and optical properties so that they can be used in different optical areas, like photodetectors.

## 2. MATERIALS AND METHODS

To investigated the (PEO/SnO<sub>2</sub>/ZrO<sub>2</sub>) nanocomposites, 30 mL of distilled water added 1 gm of PEO with continuous magnetic stirrer for 30 minutes and temperature 70°C to ensure more homogenous solution and then added (0, 2, 4 and 6) wt.% from SnO<sub>2</sub> and ZrO<sub>2</sub> NPs to PEO solvent completely. The casting method was used to prepare of (PEO/SnO<sub>2</sub>/ZrO<sub>2</sub>) nanocomposites. The Olympus (Top View) type (Nikon 73346) with an automatically controlled camera under a (10 x) magnification was employed to define the films' surface for the examined surface film. using spectrophotometer (UV-1800 <sup>0</sup>A-Shimadzu) to investigate the optical measurements.

The coefficient of absorption ( $\alpha$ ) is provided as Eq. (1) [35]:

$$\alpha = 2.303 * A/d \quad (1)$$

The absorbance is denoted by A and the sample thickness is measured by d. The photon energy ( $h\nu$ ) and the  $\alpha$  are dependent on the indirect  $E_g^{opt}$ , as demonstrated in the Eq. (2) [36].

$$ah\nu = B(h\nu - E_g^{opt} \pm E_{ph})^r \quad (2)$$

The band tailing parameter B and the type of optical transition r for the materials being studied are defined by the equation (r = 2 for permissible indirect transitions). The formula for the refraction index is Eq. (3) [37].

$$n = \frac{1 + R^{\frac{1}{2}}}{1 - R^{\frac{1}{2}}} \quad (3)$$

Indicate R represent the reflectance, the extinction coefficient (k) is illustrate by Eq. (4) [38].

$$k = \frac{\alpha\lambda}{4\pi} \quad (4)$$

$\lambda$  indicate the wavelength. The component real ( $\epsilon_1$ ) and imaginary ( $\epsilon_2$ ) parts of dielectric constant are assumed by Eqs (5) and (6) [38].

$$\epsilon_1 = n^2 - k^2 \quad (5)$$

$$\epsilon_2 = 2nk \quad (6)$$

The conduction for the optical ( $\sigma_{op}$ ) is definite by Eq. (7) [39].

$$\sigma_{opt.} = \alpha nc/4\pi \quad (7)$$

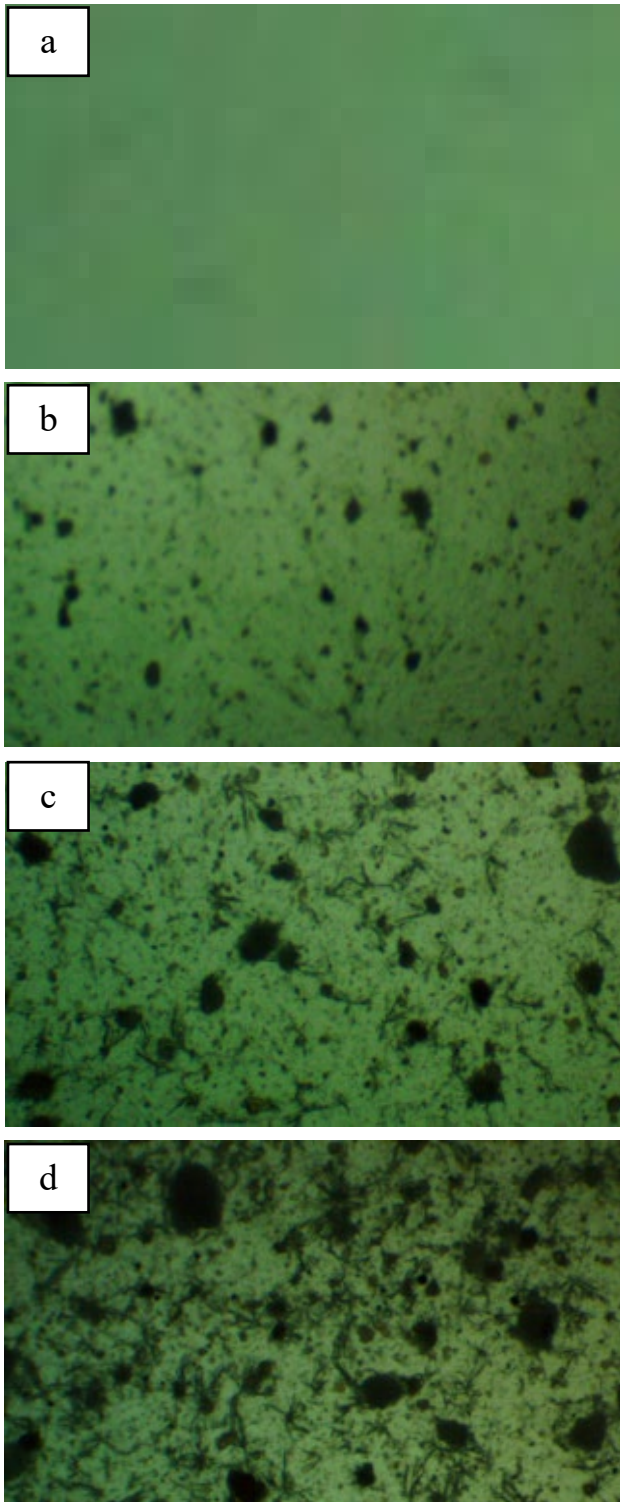
c indicates to the speed of light.

## 3. RESULTS AND DISCUSSION

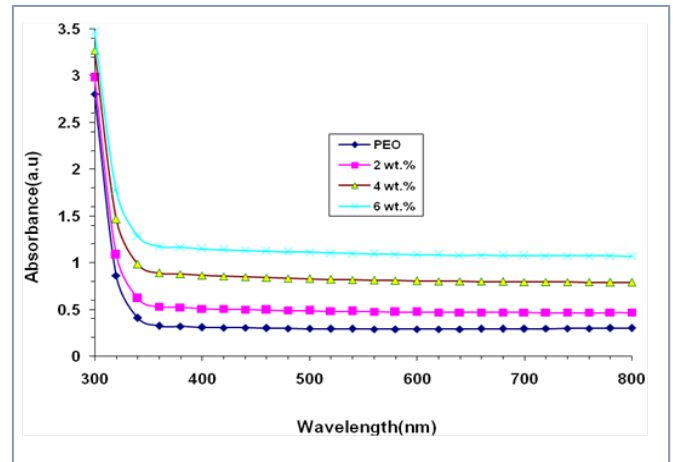
The optical microscope (OM) reveals changes in the surface morphology of (PEO-SnO<sub>2</sub>-ZrO<sub>2</sub>) nanocomposites. Figure 1 depicts the optical microscope of the (PEO-SnO<sub>2</sub>-ZrO<sub>2</sub>) nanocomposites at a 10 x magnification. Image (A) depicts a homogeneous phase with no phase separation. The image (B-E) in Figure 1 unambiguously illustrates the homogeneous dispersion of SnO<sub>2</sub> and ZrO<sub>2</sub> NPs on the PEO polymer film's surface. However, at lower concentrations, the SnO<sub>2</sub> and ZrO<sub>2</sub> NPs incline to collective and formula collections. Increasing the concentrations of SnO<sub>2</sub> and ZrO<sub>2</sub>NPs in the PEO polymer results in the formation of a network of pathways within the PEO. These pathways allow charge carriers to flow, causing a modification in the material characteristics, which can be observed. This process offered an appropriate approach for fabricating nanocomposite films. This behavior is consistent with [40-47].

Figure 2 shows the correlation between the wavelength and the absorbance characteristics of nanocomposites made of (PEO-SnO<sub>2</sub>-ZrO<sub>2</sub>). Because they have a lot of energy, photons can connect with atoms and help electrons move from lower to higher energy levels. This is the reason why all of the samples absorb a lot of ultraviolet (UV) light. This is because the photons coming in don't have enough energy to interact successfully with the material's atoms, which is why the

nanocomposite's spectra show less absorption in the near-infrared range. The screen absorption effect is more noticeable at shorter wavelengths and less noticeable as the wavelength gets longer. The absorbing effect is directly linked to the amount of SnO<sub>2</sub> and ZrO<sub>2</sub> nanoparticles present. It has also been seen that the number of charge bearers has increased. While impurity atoms are present between the conduction and valence bands, they cause a distribution of energy levels that explains the observed behaviors [48-52]. This result agrees with the researches of Kock et al. [53] and Jasim et al. [54].

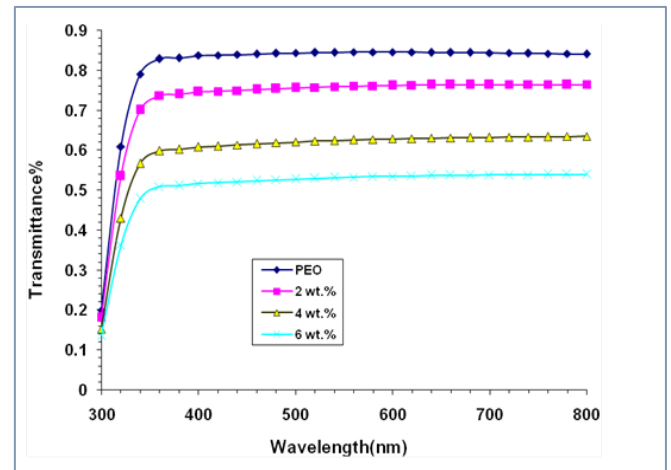


**Figure 1.** Photomicrographs for (PEO-SnO<sub>2</sub>-ZrO<sub>2</sub>) nanocomposites: (a) for (PEO) blend; (b) for 2 wt.% SnO<sub>2</sub> and ZrO<sub>2</sub> NPs; (c) for 4 wt.% SnO<sub>2</sub> and ZrO<sub>2</sub> NPs; (d) for 6 wt.% SnO<sub>2</sub> and ZrO<sub>2</sub> NPs



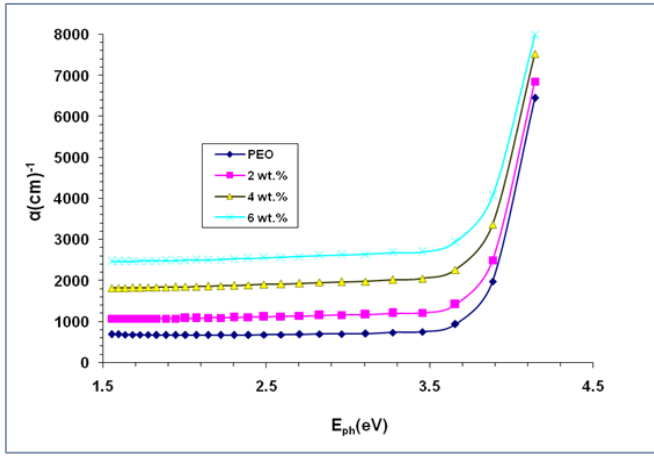
**Figure 2.** Absorbance of (PEO-SnO<sub>2</sub>-ZrO<sub>2</sub>) nanocomposites varies with wavelength

Figure 3 shows the correlation between the wavelength and the transmittance spectra of films made of (PEO-SnO<sub>2</sub>-ZrO<sub>2</sub>). Graphs of spectra showing varying concentrations of SnO<sub>2</sub> and ZrO<sub>2</sub> nanoparticles are displayed. The graph clearly shows that the transmittance decreases as the concentrations of SnO<sub>2</sub> and ZrO<sub>2</sub> increase. The capacity of the electrons in the outermost shells of SnO<sub>2</sub> and ZrO<sub>2</sub> to absorb the electromagnetic energy of the incident light and migrate to higher energy levels explains the observed behaviors. The material can absorb all incoming light and block its transmission because the moving electron occupies energy locations in each band [55].



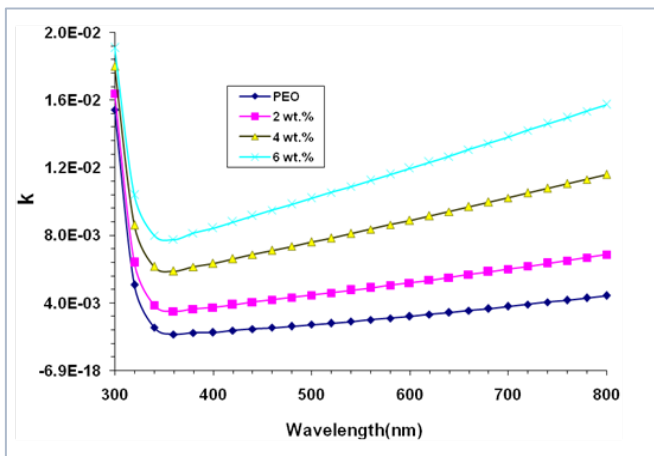
**Figure 3.** Nanocomposites of (PEO-SnO<sub>2</sub>-ZrO<sub>2</sub>) and how their transmittance spectra change with wavelength

Figure 4 shows how photon energy affects (PEO-SnO<sub>2</sub>-ZrO<sub>2</sub>) nanocomposites' absorption coefficient. As wavelengths grow and energy decrease, absorption coefficients visually decrease. Low energy photons ( $h\nu < E_g$ ) are unlikely to produce electron displacement, as per reference [56]. This study shows how absorption coefficient affects electron transition. We expect the absorption coefficient to exceed  $10^4 \text{cm}^{-1}$  at high energies. Electrons and photons conserve energy and momentum during direct electron transitions. In contrast, at low energy levels, the absorption coefficient is about  $10^4 \text{cm}^{-1}$ , indicating indirect transitions where phonons boost electric momentum [57]. PEO-SnO<sub>2</sub>-ZrO<sub>2</sub> nanocomposites absorb below  $10^4 \text{cm}^{-1}$ . Along with previous findings, this shows an indirect electron transition.



**Figure 4.** The photon energy dependence of the absorption coefficient of (PEO-SnO<sub>2</sub>-ZrO<sub>2</sub>) nanocomposites

The extinction coefficient measures how much an electromagnetic wave's intensity drops when it travels through a material. Figure 5 shows the relationship between wavelength and the extinction coefficient graphically. Extinction coefficient values are positively correlated with SnO<sub>2</sub> and ZrO<sub>2</sub> nanoparticle concentrations, as seen in the figure. A possible explanation for the enhanced film absorbance is the presence of pollutants within the energy gap, which generate a high concentration of energy levels [58].



**Figure 5.** Distinction between the extinction coefficient and wavelength of (PEO-SnO<sub>2</sub>-ZrO<sub>2</sub>) nanocomposites

Figure 6 shows the wavelength-refractive index relationship. PEO-SnO<sub>2</sub>-ZrO<sub>2</sub> nanoparticles directly affect refractive index, as seen in the graphic. Doping drugs change the direction of incident rays, creating extra energy levels. This increases the strength of reflected rays, raising the refractive index. Due to low transmittance (T) in the UV, the UV has a high refractive index. According to the standard, the visible and near-infrared (IR) ranges have low refractive index values due to high transmittance (T). SnO<sub>2</sub> and ZrO<sub>2</sub> presence increases nanocomposites' density and n values [59-63].

The energy gaps for permissible and forbidden indirect transitions are shown in Figures 7 and 8. Draw a linear line from the curve peak to the x-axis at  $(\alpha h\nu)^{1/2} = 0$  to get the allowed energy gap. Conversely, the forbidden energy gap is identified when  $(\alpha h\nu)^{1/3}$  is zero. Observations show that SnO<sub>2</sub> and ZrO<sub>2</sub> nanoparticles lower energy gaps. Doping creates energy levels within the energy gap, causing the decline. After

leaving the valence band, electrons proceed to the energy gap's local levels and then to the conduction band [64-68].

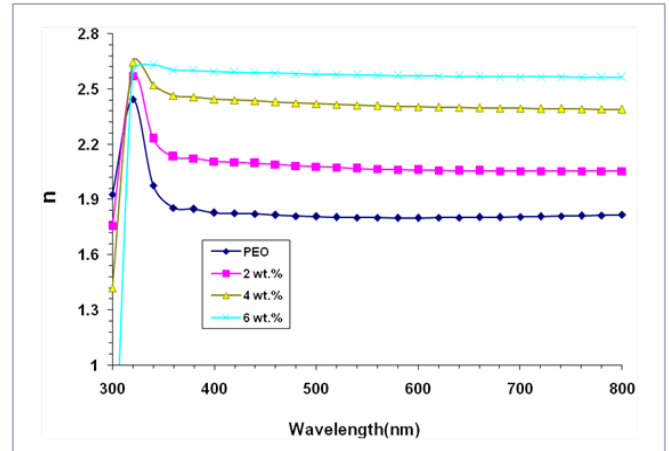


**Figure 6.** Fluctuations of the refractive index of (PEO-SnO<sub>2</sub>-ZrO<sub>2</sub>) nanocomposites as a function of wavelength

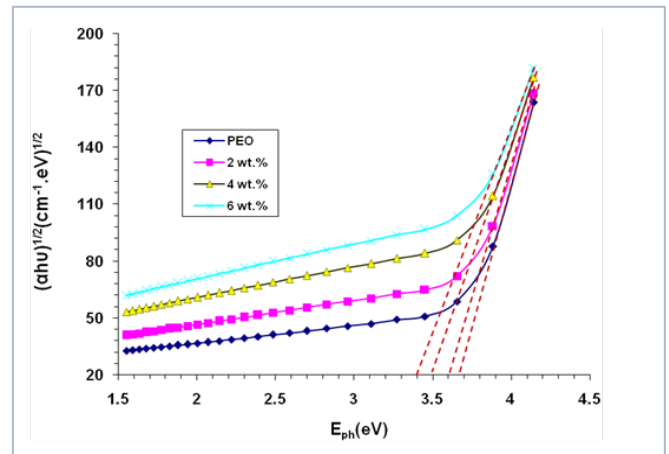


**Figure 7.** Division of  $(\alpha h\nu)^{1/2}$  for (PEO-SnO<sub>2</sub>-ZrO<sub>2</sub>) nanocomposites with photon energy

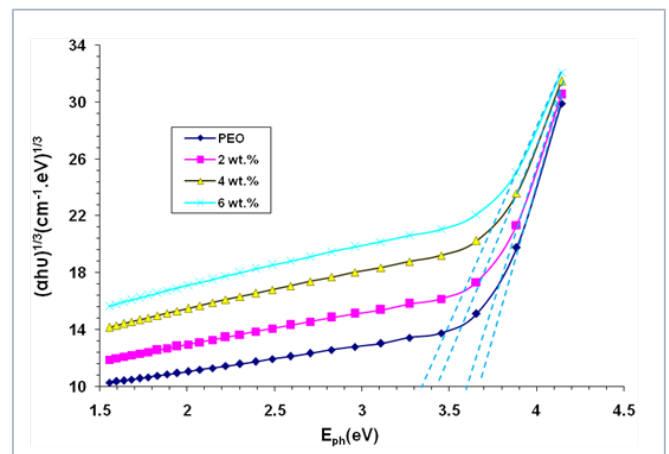


**Figure 8.** Division of  $(\alpha h\nu)^{1/3}$  for (PEO-SnO<sub>2</sub>-ZrO<sub>2</sub>) nanocomposites with photon energy

A substance's dielectric constant measures its electromagnetic radiation-induced polarization. The phenomenon is commonly described using two components: the real ( $\epsilon_1$ ) and imaginary ( $\epsilon_2$ ) dielectric constants. PEO-SnO<sub>2</sub>-ZrO<sub>2</sub> nanocomposites' real and imaginary dielectric



constants vary with wavelength, as shown in Figures 9 and 10. The study found a correlation between SnO<sub>2</sub> and ZrO<sub>2</sub> nanoparticle proportions and real and imaginary dielectric constants. Nanoparticles increase electric polarization, explaining the observed behavior. Electric polarization increases dipole concentration and dielectric constant. The true dielectric constant curves in Figure 8 closely mirror the refractive index curves, demonstrating a significant link. The refractive index (n) affects the dielectric constant more than the extinction coefficient (k), especially when squared, explaining the observed resemblance. Figure 9 shows the wavelength-hypothetical dielectric constant correlation. In the infrared and visible bands, the restraining coefficient affects the imaginary component of the dielectric constant. Despite the refractive index being roughly constant in the defined sites, the extinction coefficients increase with longer wavelengths [69].

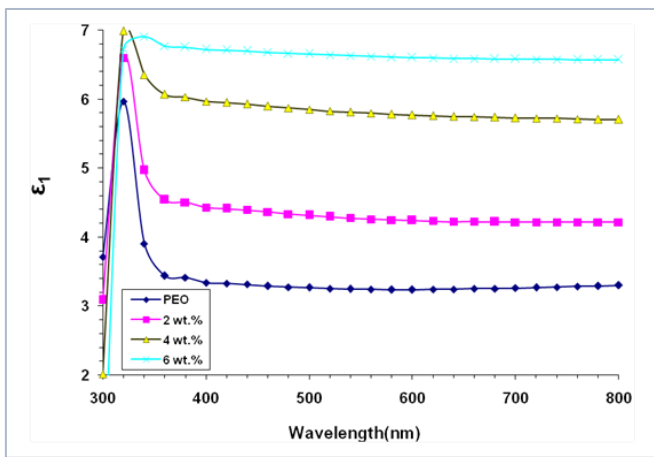


**Figure 9.** Experimental results of the dielectric constant for nanocomposites of for (PEO-SnO<sub>2</sub>-ZrO<sub>2</sub>) with wavelength

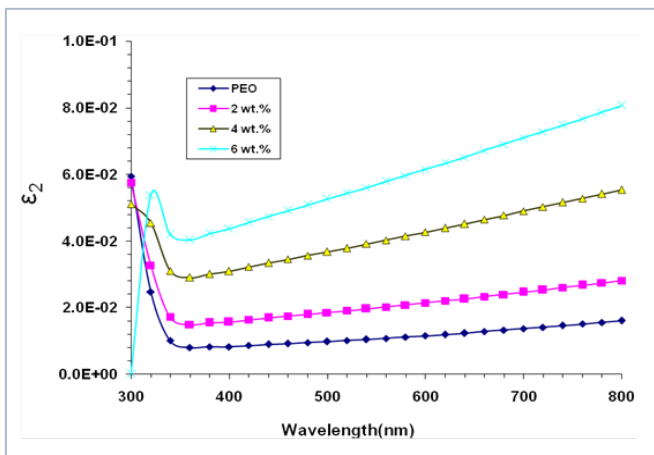


**Figure 10.** Presentation of (PEO-SnO<sub>2</sub>-ZrO<sub>2</sub>) nanocomposites with wavelength imaginary part of dielectric constant

The optical conductivity of PEO-SnO<sub>2</sub>-ZrO<sub>2</sub> nanocomposites is shown in Figure 11. All nanocomposite samples show a decrease in optical conductivity with increasing wavelength and an increase at shorter wavelengths. All nanocomposite materials absorb more light in this range, which explains their increased optical conductivity at shorter photon wavelengths. This causes charge transfer excitations to rise. Visible and near-infrared light transmission is high in the

spectrum data. Furthermore, optical conductivity is directly related to SnO<sub>2</sub> and ZrO<sub>2</sub> nanoparticle concentration. Energy gaps create specific energy levels, causing this occurrence [70-74].

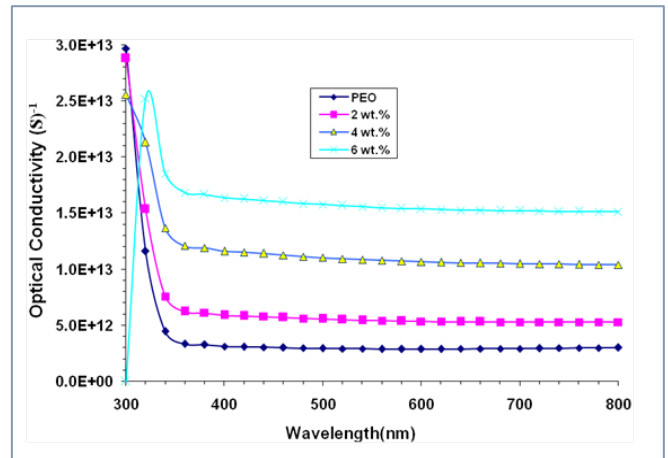


**Figure 11.** Disparity of optical conductivity for (PEO-SnO<sub>2</sub>-ZrO<sub>2</sub>) nanocomposites with wavelength

#### 4. CONCLUSIONS

The present study cast (PEO-SnO<sub>2</sub>-ZrO<sub>2</sub>) nanocomposites films. With increasing nanoparticle concentrations, optical microscope (OM) pictures showed electrically charged channels inside the polymeric matrix. PEO-SnO<sub>2</sub>-ZrO<sub>2</sub> nanocomposites have increased UV absorption based on their optical characteristics. Nanocomposites with this behavior show potential for optoelectronics. Increases in the quantities of SnO<sub>2</sub> and ZrO<sub>2</sub> nanoparticles lead to an increase in the optical conductivity, refractive index, extinction coefficient, absorbance, and real and imaginary dielectric constants of the resulting nanocomposites. The transmittance of these nanocomposites decreases proportionally with nanoparticle concentration. Both allowed and disallowed indirect transitions have a lower optical energy gap at 6wt.%. For authorized transitions, the energy gap reduces from 3.68 to 3.4 eV, and for banned transitions, from 3.66 to 3.35. Many optoelectronic device manufacturers benefit from the energy band gap reduction.

#### ACKNOWLEDGMENT

Acknowledgement to University of Babylon.

#### REFERENCES

- [1] Sasani, N., Houshyar Sadeghian, M., Khadivi, H., Golestanipour, M. (2015). A novel, simple and cost effective al a356/al2o3 nano-composite manufacturing route with uniform distribution of nanoparticles. *International Journal of Engineering*, 28(9): 1320-1327.
- [2] Akamatsu, K., Takei, S., Mizuhata, M., Kajinami, A., Deki, S., Takeoka, S., Fujii, M., Hayashi, S., Yamamoto, K. (2000). Preparation and characterization of polymer thin films containing silver and silver sulfide nanoparticles. *Thin Solid Films*, 359(1): 55-60. [https://doi.org/10.1016/S0040-6090\(99\)00684-7](https://doi.org/10.1016/S0040-6090(99)00684-7)

- [3] Mohammed, M.K., Abbas, M.H., Hashim, A., Rabee, R.H., Habeeb, M.A., Hamid, N. (2022). Enhancement of optical parameters for PVA/PEG/Cr2O3 nanocomposites for photonics fields. *Revue des Composites et des Matériaux Avancés-Journal of Composite and Advanced Materials*, 32(4): 205-209. <https://doi.org/10.18280/rcma.320406>.
- [4] Hayder, N., Hashim, A., Habeeb, M.A., Rabee, B.H., Hadi, A.G., Mohammed, M.K. (2022). Analysis of dielectric properties of PVA/PEG/In<sub>2</sub>O<sub>3</sub> nanostructures for electronics devices. *Journal of Composite & Advanced Materials/Revue des Composites et des Matériaux Avancés*, 32(5). <https://doi.org/10.18280/rcma.320507>
- [5] Rehim, M.H.A., Alhamidi, J. (2018). TiO<sub>2</sub>/polymer nanocomposites for antibacterial packaging applications. *Journal of Advancements in Food Technology*, 1(1): 1-8. <https://doi.org/10.15744/2639-3328.1.101>
- [6] Ahmed, K.K., Muheddin, D.Q., Mohammed, P.A., Ezat, G.S., Murad, A.R., Ahmed, B.Y., Hussien, S.A., Ahmed, T.Y., Hamad, S.M., Abdullah, O.G., Aziz, S.B. (2023). A brief review on optical properties of polymer composites: Insights into light-matter interaction from classical to quantum transport point of view. *Results in Physics*, 107239. <https://doi.org/10.1016/j.rinp.2023.107239>
- [7] Zhang, Q. (2011). Investigating polymer conformation in poly (Ethylene Oxide)(PEO) Based Systems for Pharmaceutical Applications A Raman Spectroscopic Study of the Hydration Process. <https://hdl.handle.net/20.500.12380/145919>
- [8] Farea, M.O., Abdelghany, A.M., Oraby, A.H. (2020). Optical and dielectric characteristics of polyethylene oxide/sodium alginate-modified gold nanocomposites. *RSC Advances*, 10(62): 37621-37630. <https://doi.org/10.1039/D0RA07601E>
- [9] Angot, S., Taton, D., Gnanou, Y. (2000). Amphiphilic stars and dendrimer-like architectures based on poly (ethylene oxide) and polystyrene. *Macromolecules*, 33(15): 5418-5426. <https://doi.org/10.1021/ma000079s>
- [10] D'amico, D.A., Montes, M.I., Manfredi, L.B., Cyras, V.P. (2016). Fully bio-based and biodegradable polylactic acid/poly (3-hydroxybutyrate) blends: Use of a common plasticizer as performance improvement strategy. *Polymer Testing*, 49: 22-28. <https://doi.org/10.1016/j.polymertesting.2015.11.004>
- [11] Hameed, T.A., Mohamed, F., Abdelghany, A.M., Turky, G. (2020). Influence of SiO<sub>2</sub> nanoparticles on morphology, optical, and conductivity properties of Poly (ethylene oxide). *Journal of Materials Science: Materials in Electronics*, 31(13): 10422-10436. <https://doi.org/10.1007/s10854-020-03591-5>
- [12] Jebur, Q.M., Hashim, A., Habeeb, M.A. (2019). Structural, electrical and optical properties for (polyvinyl alcohol-polyethylene oxide-magnesium oxide) nanocomposites for optoelectronics applications. *Transactions on Electrical and Electronic Materials*, 20(4): 334-343. <https://doi.org/10.1007/s42341-019-00121-x>
- [13] Hashim, A., Hadi, Q. (2017). Novel of (niobium carbide/polymer blend) nanocomposites: Fabrication and characterization for pressure sensors. *Sensor Letters*, 15(11): 951-953. <https://doi.org/10.1166/sl.2017.3892>
- [14] Hashim, A., Hadi, Q. (2018). Structural, electrical and optical properties of (biopolymer blend/titanium carbide) nanocomposites for low cost humidity sensors. *Journal of Materials Science: Materials in Electronics*, 29: 11598-11604. <https://doi.org/10.1007/s10854-018-9257-z>
- [15] Sajedi, S.A., Bagheri-Mohagheghi, M.M., Shirpay, A. (2023). PANI/SnO<sub>2</sub> nanoparticle, FTO/PET and Al/PET as hybrid nanocomposite soft electrodes synthesized by sol-gel, spray pyrolysis and thermal vacuum evaporation methods. *Bulletin of Materials Science*, 47(1): 9. <https://doi.org/10.1007/s12034-023-03081-4>
- [16] Xavier, B., Ramanand, A., Sagayaraj, P. (2012). Investigation on a facile one-pot rapid synthesis approach for developing modestly mono-dispersed and stable spherical gold nanoparticles. *Der Pharma Chemica* 2012, 4: 1467-1470.
- [17] Hashim, A., Hamad, Z.S. (2020). Synthesis of (Polymer-SnO<sub>2</sub>) nanocomposites: Structural and optical properties for flexible optoelectronics applications. *Nanosistemi, Nanomateriali, Nanotehnologii*, 18(4).
- [18] Yusoh, R., Horprathum, M., Eiamchai, P., Chindaudom, P., Aiempnanakit, K. (2012). Determination of optical and physical properties of ZrO<sub>2</sub> films by spectroscopic ellipsometry. *Procedia Engineering*, 32: 745-751. <https://doi.org/10.1016/j.proeng.2012.02.007>
- [19] Mamak, M., Coombs, N., Ozin, G.A. (2001). Mesoporous nickel-yttria-zirconia fuel cell materials. *Chemistry of Materials*, 13(10): 3564-3570. <https://doi.org/10.1021/cm001259j>
- [20] Zhang, R., Zhang, X., Hu, S. (2010). High temperature and pressure chemical sensors based on Zr/ZrO<sub>2</sub> electrode prepared by nanostructured ZrO<sub>2</sub> film at Zr wire. *Sensors and Actuators B: Chemical*, 149(1): 143-154. <https://doi.org/10.1016/j.snb.2010.06.009>
- [21] Wang, X., Zhai, B., Yang, M., Han, W., Shao, X. (2013). ZrO<sub>2</sub>/CeO<sub>2</sub> nanocomposite: Two step synthesis, microstructure, and visible-light photocatalytic activity. *Materials Letters*, 112: 90-93. <https://doi.org/10.1016/j.matlet.2013.09.001>
- [22] Zhang, X., Su, H., Yang, X. (2012). Catalytic performance of a three-dimensionally ordered macroporous Co/ZrO<sub>2</sub> catalyst in Fischer-Tropsch synthesis. *Journal of Molecular Catalysis A: Chemical*, 360: 16-25. <https://doi.org/10.1016/j.molcata.2012.03.024>
- [23] Gusmano, G., Montesperelli, G., Rapone, M., Padeletti, G., Cusmà, A., Kaciulis, S., Mezzi, A., Di Maggio, R. (2007). Zirconia primers for corrosion resistant coatings. *Surface and Coatings Technology*, 201(12): 5822-5828. <https://doi.org/10.1016/j.surfcoat.2006.10.036>
- [24] Zhang, C., Li, C., Yang, J., Cheng, Z., Hou, Z., Fan, Y., Lin, J. (2009). Tunable luminescence in monodisperse zirconia spheres. *Langmuir*, 25(12): 7078-7083. <https://doi.org/10.1021/la900146y>
- [25] Horti, N.C., Kamatagi, M.D., Nataraj, S.K., Wari, M.N., Inamdar, S.R. (2020). Structural and optical properties of zirconium oxide (ZrO<sub>2</sub>) nanoparticles: Effect of calcination temperature. *Nano Express*, 1(1): 010022. <https://doi.org/10.1088/2632-959X/ab8684>
- [26] Almehmadi, S.J., Alruqi, A.B., Alsalmah, H.A., Farea, M.O., Masmali, N.A., Al-Sulami, A.I., Al-Ejji, M., Rajeh, A. (2023). Improving the optical, photoluminescence, and electrical properties of PEO/NaAlg-WO<sub>3</sub> nanocomposites for optoelectronic and nanodielectric

- applications. *Journal of Materials Research and Technology*, 26: 2310-2318. <https://doi.org/10.1016/j.jmrt.2023.08.044>
- [27] Al-Harbi, L.M., Alsulami, Q.A., Farea, M.O., Rajeh, A. (2023). Tuning optical, dielectric, and electrical properties of Polyethylene oxide/Carboxymethyl cellulose doped with mixed metal oxide nanoparticles for flexible electronic devices. *Journal of Molecular Structure*, 1272: 134244. <https://doi.org/10.1016/j.molstruc.2022.134244>
- [28] Hashim, A., Abbas, M.H., Al-Aaraji, N.A.H., Hadi, A. (2023). Controlling the morphological, optical and dielectric characteristics of PS/SiC/CeO<sub>2</sub> nanostructures for nanoelectronics and optics fields. *Journal of Inorganic and Organometallic Polymers and Materials*, 33(1): 1-9. <https://doi.org/10.1007/s10904-022-02485-9>
- [29] Hashim, A., Abbas, M.H., Al-Aaraji, N.A.H., Hadi, A. (2023). Facile fabrication and developing the structural, optical and electrical properties of SiC/Y<sub>2</sub>O<sub>3</sub> nanostructures doped PMMA for optics and potential nanodevices. *Silicon*, 15(3): 1283-1290. <https://doi.org/10.1007/s12633-022-02104-9>
- [30] Hashim, A., Hadi, A., Al-Aaraji, N.A.H. (2023). Fabrication and augmented electrical and optical characteristics of PMMA/CoFe<sub>2</sub>O<sub>4</sub>/ZnCoFe<sub>2</sub>O<sub>4</sub> hybrid nanocomposites for quantum optoelectronics nanosystems. *Optical and Quantum Electronics*, 55(8): 716. <https://doi.org/10.1007/s11082-023-04994-4>
- [31] Kadhim, A.F., Hashim, A. (2023). Fabrication and augmented structural optical properties of PS/SiO<sub>2</sub>/SrTiO<sub>3</sub> hybrid nanostructures for optical and photonics applications. *Optical and Quantum Electronics*, 55(5): 432. <https://doi.org/10.1007/s11082-023-04699-8>
- [32] Hashim, A., Mohammed, B., Hadi, A., Ibrahim, H. (2024). Synthesis and augment structural and optical characteristics of PVA/SiO<sub>2</sub>/BaTiO<sub>3</sub> nanostructures films for futuristic optical and nanoelectronics applications. *Journal of Inorganic and Organometallic Polymers and Materials*, 34(2): 611-621. <https://doi.org/10.1007/s10904-023-02846-y>
- [33] Abbas, M.H., Ibrahim, H., Hashim, A., Hadi, A. (2024). Fabrication and tailoring structural, optical, and dielectric properties of PS/CoFe<sub>2</sub>O<sub>4</sub> nanocomposites films for nanoelectronics and optics applications. *Transactions on Electrical and Electronic Materials*, 1-9. <https://doi.org/10.1007/s42341-024-00524-5>
- [34] Kareem, A., Hashim, A., Hassan, H.B. (2024). Synthesis and boosting the morphological, structural and optical features of PEO/Si<sub>3</sub>N<sub>4</sub>/CeO<sub>2</sub> promising nanocomposites films for futuristic nanoelectronics applications. *Silicon*, 1-12. <https://doi.org/10.1007/s12633-024-02891-3>
- [35] Jothibas, M., Manoharan, C., Johnson Jeyakumar, S., Praveen, P. (2015). Study on structural and optical behaviors of In<sub>2</sub>O<sub>3</sub> nanocrystals as potential candidate for optoelectronic devices. *Journal of Materials Science: Materials in Electronics*, 26: 9600-9606. <https://doi.org/10.1007/s10854-015-3623-x>
- [36] Abdel-Baset, T., Elzayat, M., Mahrous, S. (2016). Characterization and optical and dielectric properties of polyvinyl chloride/silica nanocomposites films. *International Journal of Polymer Science*, 2016(1): 1707018. <https://dx.doi.org/10.1155/2016/1707018>
- [37] Agarwal, S., Saraswat, Y.K., Saraswat, V.K. (2016). Study of optical constants of ZnO dispersed PC/PMMA blend nanocomposites. *Open Physics Journal*, 3(1): 63-72. <https://doi.org/10.2174/1874843001603010063>
- [38] Micozzi, M.S., Townsend, F.M., Koop, C.E. (1990). From army medical museum to national museum of health and medicine. A century-old institution on the move. *Archives of Pathology & Laboratory Medicine*, 114(12), 1290-1295.
- [39] Tyagi, C., Devi, A. (2018). Alteration of structural, optical and electrical properties of CdSe incorporated polyvinyl pyrrolidone nanocomposite for memory devices. *Journal of Advanced Dielectrics*, 8(03): 1850020. <https://doi.org/10.1142/S2010135X18500200>
- [40] Metiab, M.H., Hashim, A., Rabee, B.H. (2023). Preparation, morphological and antibacterial activity of PS-PC/MnO<sub>2</sub>-SiC nanocomposites for biomedical applications. *Nanosistemi, Nanomateriali, Nanotehnologii*, 21(1): 199-208. <https://doi.org/10.15407/nnn.21.01.199>
- [41] Babu, J.R., Kumar, K.V. (2015). Studies on structural and electrical properties of NaHCO<sub>3</sub> doped PVA films for electrochemical cell applications. *International Journal of Chem-Tech Research*, 7(1): 2014-2015.
- [42] Metiab, M.H., Hashim, A., Rabee, B.H. (2023). Synthesis and structural properties of (PS-PC/Co<sub>2</sub>O<sub>3</sub>-SiC) nanocomposites for antibacterial applications. *Nanosistemi, Nanomateriali, Nanotehnologii*, 21(2). <https://doi.org/10.15407/nnn.21.02.451>
- [43] Metiab, M.H., Hashim, A., Rabee, B.H. (2023). Synthesis and characteristics of SiC/MnO<sub>2</sub>/PS/PC quaternary nanostructures for advanced nanodielectrics fields. *Silicon*, 15(4): 1609-1620. <https://doi.org/10.1007/s12633-022-02114-7>
- [44] Metiab, M.H., Hashim, A., Rabee, B.H. (2023). Controlling the structural and dielectric characteristics of PS-PC/Co<sub>2</sub>O<sub>3</sub>-SiC hybrid nanocomposites for nanoelectronics applications. *Silicon*, 15(1): 251-261. <https://doi.org/10.1007/s12633-022-02020-y>
- [45] Kadhim, A.F., Hashim, A. (2023). Fabrication and tuning the structural and dielectric characteristics of PS/SiO<sub>2</sub>/SrTiO<sub>3</sub> hybrid nanostructures for nanoelectronics and energy storage devices. *Silicon*, 15(11): 4613-4621. <https://doi.org/10.1007/s12633-023-02381-y>
- [46] Ahmed, G., Hashim, A. (2023). Synthesis of PMMA/PEG/Si<sub>3</sub>N<sub>4</sub> nanostructures and exploring the structural and dielectric characteristics for flexible nanoelectronics applications. *Silicon*, 15(9):3977-3985. <https://doi.org/10.1007/s12633-023-02322-9>
- [47] Kareem, A., Hashim, A., Hassan, H.B. (2024). Ameliorating and tailoring the morphological, structural, and dielectric features of Si<sub>3</sub>N<sub>4</sub>/CeO<sub>2</sub> futuristic nanocomposites doped PEO for nanoelectronic and nanodielectric applications. *Journal of Materials Science: Materials in Electronics*, 5(7): 461. <https://doi.org/10.1007/s10854-024-12278-0>
- [48] Al-Aaraji, N.A.H., Hashim, A., Hadi, A., Abduljalil, H.M. (2022). Synthesis and enhanced optical characteristics of silicon carbide/copper oxide nanostructures doped transparent polymer for optics and photonics nanodevices. *Silicon*, 14(15): 10037-10044. <https://doi.org/10.1007/s12633-022-01730-7>
- [49] Obaid, W.O., Hashim, A. (2022). Synthesis and augmented optical properties of PC/SiC/TaC hybrid nanostructures for potential and photonics fields. *Silicon*,

- 14(17): 11199-11207. <https://doi.org/10.1007/s12633-022-01854-w>
- [50] Ahmed, H., Hashim, A. (2021). Structure, optical, electronic and chemical characteristics of novel (PVA-CoO) structure doped with silicon carbide. *Silicon*, 13(12): 4331-4344. <https://doi.org/10.1007/s12633-020-00723-8>
- [51] Hazim, A., Abduljalil, H.M., Hashim, A. (2021). Design of PMMA doped with inorganic materials as promising structures for optoelectronics applications. *Transactions on Electrical and Electronic Materials*, 22(6): 851-868. <https://doi.org/10.1007/s42341-021-00308-1>
- [52] Ahmed, H., Hashim, A. (2022). Design of polymer/lithium fluoride new structure for renewable and electronics applications. *Transactions on Electrical and Electronic Materials*, 23(3): 237-246. <https://doi.org/10.1007/s42341-021-00340-1>
- [53] Kock, I., Edler, T., Mayr, S.G. (2008). Growth behavior and intrinsic properties of vapor-deposited iron palladium thin films. *Journal of Applied Physics*, 103(4). <https://doi.org/10.1063/1.2875306>
- [54] Jasim, F.A., Hashim, A., Hadi, A.G., Lafta, F., Salman, S.R., Ahmed, H. (2013). Preparation of (pomegranate peel-polystyrene) composites and study their optical properties. *Research Journal of Applied Sciences*, 8(9): 439-441. <https://doi.org/10.3923/rjasci.2013.439.441>
- [55] Anwar, M., Kayani, Z.N., Hassan, A. (2021). An insight of physical and antibacterial properties of Au-doped ZnO dip coated thin films. *Optical Materials*, 118: 111276. <https://doi.org/10.1016/j.optmat.2021.111276>
- [56] Indolia, A.P., Gaur, M.S. (2013). Optical properties of solution grown PVDF-ZnO nanocomposite thin films. *Journal of Polymer Research*, 20: 1-8. <https://doi.org/10.1007/s10965-012-0043-y>
- [57] Du, H., Xu, G.Q., Chin, W.S., Huang, L., Ji, W. (2002). Synthesis, characterization, and nonlinear optical properties of hybridized CdS-polystyrene nanocomposites. *Chemistry of materials*, 14(10): 4473-4479. <https://doi.org/10.1021/cm010622z>
- [58] Yu, S.H., Yoshimura, M., Calderon Moreno, J.M., Fujiwara, T., Fujino, T., Teranishi, R. (2001). In situ fabrication and optical properties of a novel polystyrene/semiconductor nanocomposite embedded with CdS nanowires by a soft solution processing route. *Langmuir*, 17(5): 1700-1707. <https://doi.org/10.1021/la000941p>
- [59] Narang, N., Tyagi, A.K. (2020). Structural and optical properties of ZnO and ZnO/PS core-shell nano composites. *J Univ Shanghai Sci Technol*, 22(12): 359.
- [60] Hussien, H.A.J., Hashim, A. (2023). Synthesis and exploring the structural, electrical and optical characteristics of PVA/TiN/SiO<sub>2</sub> hybrid nanosystem for photonics and electronics nanodevices. *Journal of Inorganic and Organometallic Polymers and Materials*, 33(8): 2331-2345. <https://doi.org/10.1007/s10904-023-02688-8>
- [61] Ahmed, G., Hashim, A. (2023). Synthesis and tailoring morphological and optical characteristics of PMMA/PEG/Si<sub>3</sub>N<sub>4</sub> hybrid nanomaterials for optics and quantum nanoelectronics applications. *Silicon*, 15(16): 7085-7093. <https://doi.org/10.1007/s12633-023-02572-7>
- [62] Hashim, A., Hadi, A., Abbas, M.H. (2023). Fabrication and unraveling the morphological, optical and electrical features of PVA/SnO<sub>2</sub>/SiC nanosystem for optics and nanoelectronics applications. *Optical and Quantum Electronics*, 55(7): 642. <https://doi.org/10.1007/s11082-023-04929-z>
- [63] Hussien, H.A.J., Kadhim, R.G., Hashim, A. (2022). Investigating the low cost photodegradation performance against organic Pollutants using CeO<sub>2</sub>/MnO<sub>2</sub>/polymer blend nanostructures. *Optical and Quantum Electronics*, 54(11): 704. <https://doi.org/10.1007/s11082-022-04094-9>
- [64] Hashim, A., Alshrefi, S.M., Abed, H.H., Hadi, A. (2024). Synthesis and boosting the structural and optical characteristics of PMMA/SiC/CdS hybrid nanomaterials for future optical and nanoelectronics applications. *Journal of Inorganic and Organometallic Polymers and Materials*, 34(2): 703-711. <https://doi.org/10.1007/s10904-023-02866-8>
- [65] Al-Aaraji, N.A.H., Hashim, A., Abduljalil, H.M., Hadi, A. (2023). Tailoring the design, structure and spectroscopic characteristics of SiC/CuO doped transparent polymer for photonics and quantum nanoelectronics fields. *Optical and Quantum Electronics*, 55(8): 743. <https://doi.org/10.1007/s11082-023-05048-5>
- [66] Hashim, A., Hadi, A., Al-Aaraji, N.A.H., Rashid, F.L. (2023). Fabrication and augmented structural, optical and electrical features of PVA/Fe<sub>2</sub>O<sub>3</sub>/SiC hybrid nanosystem for optics and nanoelectronics fields. *Silicon*, 15(13): 5725-5734. <https://doi.org/10.1007/s12633-023-02471-x>
- [67] J Jaafar, H.K., Hashim, A., Rabee, B.H. (2023). Fabrication and tuning the morphological and optical characteristics of PMMA/PEO/SiC/BaTiO<sub>3</sub> newly quaternary nanostructures for optical and quantum electronics fields. *Optical and Quantum Electronics*, 55(11): 989. <https://doi.org/10.1007/s11082-023-05208-7>
- [68] Kumar, U., Padalia, D., Bhandari, P., Kumar, P., Ranakoti, L., Singh, T., Lendvai, L. (2022). Fabrication of europium-Doped barium titanate/polystyrene polymer nanocomposites using ultrasonication-assisted method: Structural and optical properties. *Polymers*, 14(21): 4664. <https://doi.org/10.3390/polym14214664>
- [69] Manhas, S.S., Rehan, P., Kaur, A., Acharya, A.D., Sarwan, B. (2019). Evaluation of optical properties of polypyrrole: Polystyrene nanocomposites. In *AIP Conference Proceedings*. AIP Publishing, 2100(1). <https://doi.org/10.1063/1.5098591>
- [70] Hashim, A., Hadi, A., Abbas, M.H. (2023). Synthesis and unraveling the morphological and optical features of PVP-Si<sub>3</sub>N<sub>4</sub>-Al<sub>2</sub>O<sub>3</sub> nanostructures for optical and renewable energies fields. *Silicon*, 15(15): 6431-6438. <https://doi.org/10.1007/s12633-023-02529-w>
- [71] Kadhim, A.F., Ahmed, G., Hashim, A. (2024). Fabrication and tuning the structural and optical features of SiO<sub>2</sub>/Si<sub>3</sub>N<sub>4</sub> nanomaterials doped PS for promising optoelectronics applications. *Journal of Inorganic and Organometallic Polymers and Materials*, 1-10. <https://doi.org/10.1007/s10904-024-03075-7>
- [72] Hashim, A., Hadi, A., Ibrahim, H., Rashid, F.L. (2024). Fabrication and boosting the morphological and optical properties of PVP/SiC/Ti nanosystems for tailored renewable energies and nanoelectronics fields. *Journal of Inorganic and Organometallic Polymers and Materials*, 34(4): 1678-1688. <https://doi.org/10.1007/s10904-023-02908-1>



[73] Mondal, K.G., Jana, P.C., Saha, S. (2023). Optical and structural properties of 2D transition metal dichalcogenides semiconductor MoS<sub>2</sub>. Bulletin of Materials Science, 46(1): 15. <https://doi.org/10.1007/s12034-022-02852-9>

[74] Fadil, O.B., Hashim, A. (2022). Fabrication and tailored optical characteristics of CeO<sub>2</sub>/SiO<sub>2</sub> nanostructures doped PMMA for electronics and optics fields. Silicon, 14(15): 9845-9852. <https://doi.org/10.1007/s12633-022-01728-1>